Adaptation of acidogenic sludge to increasing glycerol concentrations for biohydrogen production

Estela Tapia-Venegas, L. Cabrol, B. Brandhoff, Jérôme Hamelin, Eric Trably, Jean-Philippe Steyer, G. Ruiz-Filippi

Adaptation of acidogenic sludge to increasing glycerol concentrations for bio-hydrogen production

E. Tapia[1*], L. Cabrol[1,2], B. Brandhoff[1], J. Hamelin[3], E. Trably[3], JP Steyer[3], G. Ruiz-Filippi[1]

[1] *Escuela de Ingeniería Bioquímica, Pontificia Universidad Católica de Valparaíso*, Avenida Brasil 2085, Valparaíso, Chile.

[2]Fraunhofer Chile Research Foundation – Center for Systems Biotechnology, FCR-CSB. Mariano Sánchez Fontecilla 310, Las Condes, Santiago, Chile

[3]INRA, UR 0050, Laboratoire de Biotechnologie de l'Environnement, Avenue des Etangs F-11100, Narbonne, France.

*****Corresponding author. Escuela de Ingeniería Bioquímica, Pontificia Universidad Católica de Valparaíso, Av Brasil 2085, Valparaíso, Chile. Tel.: +56 (32)2372025*

Abstract

Hydrogen is a promising alternative as energetic carrier and its production by dark fermentation from wastewater has been recently proposed, with special attention to crude glycerol as potential substrate. In this study, two different feeding strategies were evaluated for replacing the glucose substrate by glycerol substrate: a one-step strategy (glucose was replaced abruptly by glycerol) and a step-by-step strategy (progressive decrease of glucose concentration and increase of glycerol concentration from 0 to 5g.L^{-1}), in a continuous stirred tank reactor (12h of HRT, pH 5.5, 35°C). While the one-step strategy led to biomass washout and unsuccessful H_2 production, the step-by-step strategy was efficient for biomass adaptation, reaching acceptable hydrogen yields (0.4 ± 0.1 $mol_{H2}.mol^{-1}_{glycerol\ consumed}$) around 33% of the theoretical yield independently of the glycerol concentration. Microbial community structure was investigated by SSCP and DGGE fingerprinting techniques, targeting either the total community (16S) or the functional clostridium population involved in H_2 production (hydA gene), as well as by 454 pyrosequencing of the total community. Multivariate analysis of fingerprinting and pyrosequencing results revealed the influence of the feeding strategy on the bacterial community structure and suggested the progressive structural adaptation of the community to increasing glycerol concentrations, through the emergence and selection of specific species, highly correlated to environmental parameters. Particularly, this work highlighted an interesting microbial succession according to the gradient of glycerol proportion in the feed, with successive dominance of *Veillonellaceae, Prevotella* and *Clostridium sp*, putatively responsible of hydrogen production in the CSTR under different glycerol concentration.

Keywords: Acidogenic sludge adaptation, biohydrogen, glycerol, dark fermentation, community structure, pyrosequencing

Introduction

Hydrogen is an energetically promising alternative, mainly because it is an energetic vector that allows the generation of electric energy with high efficiency, has high calorific value per weight unit and its combustion in presence of oxygen only emits water vapour (Lattin et al., 2007; Niu et al., 2010). There is a high variety of hydrogen producing technologies that require the use of external non-renewable energy, representing a strong economical and environmental disadvantage (Elam et al., 2003). Hydrogen can also be produced by biological fermentation process, through the use of microorganisms. Dark fermentation is one of the most attractive biological processes compared to photofermentation because a variety of carbon sources can be used as substrates and its production is performed continuously without depending on solar energy (Das et al. 2008; Guo et al., 2010). Hydrogen production through dark fermentation from wastewaters is environmentally sustainable and economically attractive since it allows both energy recovery and waste mitigation (Khanal et al., 2004).

During the last decade, glycerol generation as by-product of biodiesel production has significantly increased, the annual growth of biodiesel market being estimated to reach 42% by 2016 (Yang et al., 2013; Siles et al., 2009). Therefore, crude glycerol production exceeds the current commercial demand of purified glycerol since the last decade and has been recently proposed as carbon source for bioenergy production (Singhabhandhu et al., 2010). It is a potential promising feedstock for hydrogen production, since it is a simple substrate that is easily biodegradable during glycolysis by an oxidative pathway. Moreover, it is an abundant industrial by-product (Siles et al., 2010; Varrone et al., 2013;).

Several glycerol degradation routes producing hydrogen as co-product have been suggested, including ethanol, acetate, butyrate and formate pathways, but they have still not been clearly elucidated (Da Silva et al., 2009; Trchounian et al., 2009). Most of previous studies have used pure microbial cultures such as *Enterobacter aerogenes*, obtaining yields from 0.69 to 0.89 $mol_{H2}mol^{-1}_{glycerol}$ (Ito et al., 2005; Sakai et al., 2007; Akutsu et al., 2009; Markov et al., 2011; Wu et al., 2011). However, to make the process economically profitable, operation costs must be lowered, for instance by working under non-sterile conditions and using mixed microbial cultures. A limited diversity of adapted microorganisms can be selected by specific operating conditions, such as the type of substrate (Ito et al., 2005; Seifert et al., 2009) or the hydraulic retention time (HRT). When mixed cultures coming from anaerobic digester were used in continuous systems with low HRT, low hydrogen yields were reported (0.05 $mol_{H2}mol^{-1}_{glycerol}$), although higher yields were observed after inoculum pretreatment through thermal shock (0.11-0.41 $mol_{H2}mol^{-1}_{glycerol}$) (Temudo et al., 2008). This type of pretreatment is unsuitable at industrial scale because it implies an extra energetic cost and a lack of robustness of the biomass to face operational failures (Ren et al., 2008; Akutsu et al., 2009; Seifert et al., 2009; Varrone et al., 2012). Therefore, it is interesting to study a glycerol adaptation strategy of the mixed culture without a pretreated inoculum.

The success of biohydrogen production strongly depends on species composition and interactions within the bacterial community (Rafrafi et al., 2013). Investigation of the dynamics of the microbial community diversity

in mixed cultures provides new insights to understand the community-level adaptations, that could help controlling the process stability (Tolvanen et al., 2011; Cabrol and Malhautier, 2011; Pu et al., 2014). Despite some well-known methodological biases (e.g. preferential amplification, co-migration of different species, multiple copies of the targeted gene with different sequences) (Muyzer and Smalla; 1998), fingerprinting techniques such as PCR-DGGE and PCR-SSCP are useful to rapidly evidence changes in community structure of dominant species associated with operating and/or functional changes in hydrogen-producing reactors (Tolvenen et al., 2011; Rafrafi et al., 2013). In addition, next generation high-throughput sequencing tools provide deeper characterization of the community including minor species (Goud et al., 2012; Laothanachareon et al., 2014), which are known to play key functional role in hydrogen production (Rafrafi et al., 2013).

The analysis of key functional genes involved in H_2 production is a smart process monitoring tool, enabling to adjust operating parameters during the operation so as to enhance the growth of targeted microorganisms responsible for hydrogen production (Chen et al., 2006; Tolvanen et al., 2011).Given that the most abundant hydrogen producers have been mainly affiliated to *Clostridium* genus, special attention has been paid to monitor the abundance and diversity of clostridial *hydA* gene coding for the Fe-Fe hydrogenase enzyme, through the development and validation of specific primers (Quéméneur et al. 2010). Several authors reported the strong correlation between the hydrogen production performance and the abundance and expression level of clostridial hydrogenase (Chang et al., 2006; Quéméneur et al., 2011; Chen et al., 2011; Winkler et al., 2013)

With the purpose of broadening the range of potential substrates for hydrogen production, we evaluated the conversion of glycerol to hydrogen, using anaerobic sludge (previously adapted to glucose) in chemostat operated at low HRT without thermal pretreatment. The aim of this work is to study the adaptation of the biomass to glycerol substrate, according to different strategies, either a one-step strategy (abrupt substrate change from glucose to glycerol) or a step-by-step strategy (progressive increase of glycerol concentration).The adaptation process was evaluated at both functional and microbial levels, in order to assess the relationships between operating conditions, functional performance and community structure.

I. Material and methods

2.1 Operating conditions and experimental design

Experiments were carried out in a 2 L (working volume) continuous stirred tank reactor (CSTR), under anaerobic conditions. pH and temperature were controlled and maintained at, 5.5 and 37 °C, respectively and the agitation rate was maintained at 240 rpm. The reactor was inoculated at 4 $g_{VSS}.L^{-1}$ with a sludge from a granular anaerobic digester. The hydraulic retention time (HRT) was set at 12 h as previously reported by Tapia-Venegas *et al*. (2013).

Two different feeding strategies were evaluated for replacing glucose by glycerol substrate (table 1). In the one-step strategy, glucose was replaced abruptly by glycerol and feeding at glycerol concentration of 5.2 ± 0.1 $g.L^{-1}$ from day 0. In the step-by-step strategy, after an initial glucose-feeding phase at 5.1 ± 0.3 $g.L^{-1}$ (stage 0), the

reactor was fed with a mixture of glucose (at 2.4 ± 0.1 $g.L^{-1}$) and glycerol at increasing concentrations (from 2.0 ± 0.1 $g.L^{-1}$ to 5.0 ± 0.1 $g.L^{-1}$) during stages 1 to 4 (Table 1). Finally, the reactor was fed only with glycerol at 5.0 ± 0.1 $g.L^{-1}$ (stage 5). The synthetic feeding medium was supplemented with salts and minerals according to Tapia-Venegas *et al*., 2013. Every stage was maintained for approximately 20 HRTs after reaching a steady state in terms of hydrogen yield (i.e. once the relative standard deviation of H_2 yield was kept around 21 % on average).

2.3 Chemical analysis

Chemical oxygen demand (COD) and volatile suspended solids (VSS) were measured according to Standard Method 5220D. Glucose was measured by dinitrosalicylic acid method and glycerol by HPLC (Biorad HPX-87-H column, Bio-Rad Laboratories, Hercules, CA, US). Volatile fatty acids (VFA) and ethanol were quantified by gas chromatography: A GC-8A (Shimadzu, Kyoto, Japan) measurement, equipped with an ID GP 60/80 Carbopack C/0.3 % Carbowax 20 M/0.1 % H_3PO_4 packaged column (Sigma Aldrich, St Louis, MO, US) and a Clarus 500 chromatograph (Perkin Elmer, Waltham, MA, US) was used, equipped with a Wide bore, Semi-capillary, Equity 1 column (Sigma-Aldrich, St. Louis, MO, US), respectively. The biogas flow was measured by water displacement and the biogas composition was determined by gas chromatography in a Perkin Elmer Clarus 500 chromatograph equipped with a Hayesep Q 4 m x 1/8"OD column (VICI, Bandera, TX, US).

2.4 Bacterial community characterization

Biomass samples were collected and were centrifuged at 10.000 rpm for 10 min. Total genomic DNA was extracted from the pellet using Power Soil DNA isolation kit (MO BIO Laboratories, Carlsbad, CA, USA) and stored at -20 °C before use.

The V3 region from the ribosomal 16S DNA (around 200 bp) was amplified by PCR for DGGE and SSCP analysis, using Immolase DNA-Polymerase (Bioline, London, UK) and *Pfu* Turbo DNA polymerase (Stratagene) anda 5'-fluorescein phosphoramidite labeled reverse primer, respectively, with w49F and w104R bacterial primers. A 40 bp GC-clamp was added at the 5' end of the forward primer to perform the DGGE analysis. The PCR products with GC-clamp (500 ng) were separated through denaturing gradient gel electrophoresis (DGGE) on a 10 % polyacrylamide gel with a linear gradient ranging from 20 % to 70 %, using the DCode™ Universal Mutation Detection System (BioRad Laboratories Inc, Hercules, CA, US) and the gels were stained with SYBR®Green (Invitrogen, Life Technology, Carlsbad, CA, US) and photographed for further analysis. The PCR products without GC-clamp were diluted (5- to 2000-fold diluted) and 1 µL was mixed with 18.8 µL of formamide and 0.2 µL of internal standard Gene Scan ROX (Applied Biosystems, Foster City, CA, US). Samples were heat denatured at 95 °C for 5 min and immediately cooled in ice. SSCP electrophoresis was performed in an ABI Prism 3130genetic analyser (Applied Biosystems) with 50-cm long capillary tubes filled with a non-denaturing 5.6 % conformation analysis polymer (Applied Biosystems). Samples were eluted at 12 kV and 32 °C for 30 min.

A fragment of the *hydA* gene (around 250 bp) coding for clostridial Fe-Fe hydrogenase was amplified by PCR for DGGE and SSCP analysis using Platinum Taq-DNA-Polymerase (Invitrogen, Life Technology, Carlsbad, CA, US) and *Pfu* Turbo DNA polymerase (Stratagene) and a 5'-fluorescein phosphoramidite labeled reverse primer, respectively, with hydA-F and hydA-R primers (Quéméneur *et al*., 2011). *PCR_DGGE*: Three PCR were carried out in parallel and the PCR products were mixed and concentrated through the use of the gel/PCR purification mini kit (Favorgen Biotech Corp, Ping-Tung, Taiwan). The PCR products were separated by DGGE using the same protocol as previously described for 16S gene amplicons, excepted that a 8 %-polyacrylamide gel was used. *PCR-SSCP:* The PCR products were separated by SSCP using the same protocol as previously described for 16S gene amplicons, the only difference being that samples were eluted at 12 kV and 32 °C for 64 min.

Genomic DNA were sent to Molecular Research Laboratory (Shallowater, TX, US) for determination of the community composition using 454-pyrosequencing of the V4-V5 regions of the 16S rRNA gene which captures most of the bacterial and archaeal diversity (Wang and Qian 2009).

2.5 Numerical and statistical analysis

Each metabolite concentration was converted to COD and expressed in percentage of total measured metabolites. The hydrogen yield was calculated in $mmol_{H2}.gCOD^{-1}_{consumed}$. Hydrogen yield was also expressed as a percentage of the theoretical yield when comparing the different substrates. The theoretical yield for each intermediary stage was calculated as a combination of the theoretical H_2 yields of pure glucose (4 $mol_{H2}.mol^{-1}_{glucose\ consumed}$) and glycerol (1 $mol_{H2}.mol^{-1}_{glycerol\ consumed}$), weighted by their respective proportions in the feeding mixture (Ito *et al.*, 2005; Akutsu *et al.*, 2009).

DGGE profiles were aligned and analyzed with GelCompar II software (Applied Maths, Sint-Martens-Latem, Belgium), to obtain the matrix of relative band intensity according to band position. The DGGE band intensities were normalized by profile before further analysis.

Raw SSCP data were aligned with the internal standard ROX to correct any change in the electrophoretic motility between run sand SSCP peak areas were normalized before statistical analysis with the *Stat Fingerprints* library from R (R Development Core Team 2009).

All band- or peak-intensity matrices from (respectively) DGGE and SSCP analyses were further computed using R software. The pair-wise similarity between community profiles was calculated by the Bray-Curtis index and the samples were clustered by UPGMA dendrogram using the *cluster* library. Principal Compoment Analysis (PCA) was computed with the *vegan* library. Correlations between the bacterial community structure and various (normalized) environmental variables (EV) were investigated by fitting the EV onto the ordination (*envfit* function from *vegan*). The significance was tested by a permutation test. The most discriminant EV (p-value < 0.05) were represented on the PCA plot as arrows whose direction and length indicate, respectively, (i) the direction of the increasing EV gradient and (ii) the magnitude of the correlation between the EV and the

ordination. Moreover, a bubble representation was superimposed on the PCA plot, by allocating to each sample a symbol size proportional to the percentage of glycerol in the feed at the corresponding sampling date.

Raw 454-pyrosequencing data were processed through the Mothur pipeline. Sequence data were first trimmed to remove the sequences containing wrong barcodes or primers, as well as the sequences shorter than 200 bp and those containing long homopolymers. Putative chimeras were removed with the *uchime* function of Mothur. Finally, 38.812 high-quality sequences were conserved from the initial data set. Sequences were aligned against the Silva v119 database. Sequences were grouped in OTUs at 97 % similarity level, resulting in 593 different OTUs. The OTU abundances were standardized for each sample before further analysis. Taxonomic affiliation up to the genus level was realized using Mothur by comparison with the Silva v119 database. To assign the sequences at the species level, a BLAST analysis was carried out. PCA was computed on standardized OTU abundance table using the same procedure as for fingerprinting patterns. The discriminant OTUs displaying most of the variance in community ordination were identified by the *envfit* function from *vegan*. The fitting relationship significance was tested by a permutation test. The 20 most abundant OTUs were represented on the PCA plot as arrows and the most discriminant ones (p-value < 0.05) were highlighted in bold.

3. Results

3.1 Glycerol degradation efficiency and biomass yield

With the one-step strategy, as a control, the microorganisms coming from the anaerobic sludge inoculum were rapidly washed out of the reactor, not being able to degrade glycerol under the present conditions.

With the step-by-step strategy, the glycerol degradation efficiency increased from 52.8 ± 3.5 % (for glycerol concentrations between 2 and 3 $g.L^{-1}$), to 68.5 ± 2.7 % (for glycerol concentrations between 4 and 5 $g.L^{-1}$) (Table 2). In all stages where glucose was present in the feed, glucose degradation efficiency remained similar and high (87 ± 3.9 %).

The biomass yield in the step-by-step strategy was reduced by 53.9 % between extreme feeding conditions with glucose only (stage 0) and glycerol only (stage 5) substrates (Table 2).

3.2 Hydrogen production performance

Hydrogen productivity in the step-by-step strategy was variable according to the operation stage. The maximum productivity (61.9 ± 12.2 $ml_{H2}.L^{-1}h^{-1}$) was obtained with glucose as sole substrate at a concentration of 5.4 $g_{COD}.L^{-1}$. It decreased to 31.4 ± 3.8 % after the first substrate shift, corresponding to the addition of glycerol at 2 $g.L^{-1}$ in the mixed feed. Afterwards, hydrogen productivity increased up to 46.7 ± 10.3 % with the increase of glycerol availability in the feeding mixture from 3 to 5 $g.L^{-1}$, suggesting a progressive adaptation of the microbial community to the changing substrate mixture. However, the lowest hydrogen productivity (24.7 ± 9.1 $ml_{H2}.L^{-1}h^{-1}$) was obtained during the last stage, once glucose had been completely removed from the feed and glycerol was the sole substrate.

The hydrogen yield decreased from 6.1 ± 1.2 $mol_{H2}.g^{-1}_{COD\ consumed}$ to 4.6 ± 0.9 $mol_{H2}.g^{-1}_{COD\ consumed}$ with glucose or a mixture of glucose and glycerol as substrate, respectively (Table 2). The hydrogen yield seemed to be negatively correlated to the proportion of glycerol in the feed mixture. The lowest hydrogen yield (3.2 ± 1.1

$mol_{H2}.g^{-1}_{COD\ consumed}$) was obtained with glycerol as sole substrate, corresponding to a 50 %-loss compared to the glucose-feeding conditions. However, it is complicated to compare these yields obtained with different substrates and substrate mixtures, since glucose and glycerol have different theoretical maximal yields. The actual yield was therefore assessed as a percentage of the theoretical maximum yield (materials and methods) and appeared that the potential for producing hydrogen was maintained within a relatively close range, independently of the substrate ratio, at around 33±5 % of the theoretical yield.

The hydrogen production performances reached with the step-by-step strategy with glycerol as sole substrate were better than the ones obtained after a direct shift from glucose to glycerol without progressive transition (one step strategy), which led to unsuccessful H_2 production and a rapid biomass washout. Therefore, the stepwise increase of glycerol ratio in the feed and the progressive decrease of glucose concentration was a successful strategy for the adaptation of biomass to hydrogen production from glycerol.

3.3 By-products of hydrogen production

The main volatile fatty acids and alcohols detected as by-products of hydrogen production during the different operation stages in the step-by-step strategy are presented in Table 2. According the COD mass balance, the detected by-products represented about 85 % of the COD in the outlet of the reactor for each operation stage. Therefore, the metabolites that were not targeted by our analysis, eg. 1,3-propanediol, represented less than 15 % of the total COD.

The intermediate product distribution was very similar whatever the inlet substrate composition and concentration. The main intermediate products in all operation stages were acetate and ethanol, representing about 66 ± 8 % of the measured metabolites. Propionate and butyrate were also detected in all cases, although in lower proportions, ie. less than 27 % of the measured metabolites. Valerate was only detected when glycerol was present in the feed (stages 1 to 5), at very low concentrations (less than 10 %).

3.4 Effect of increasing glycerol concentration on total community structure

According to the UPGMA clustering based on Bray Curtis similarity from 16S DGGE profiles, the anaerobic sludge named I0 (producing methane as end-product) and used as inoculum exhibited the most different community structure, and felt clearly apart from all other stages of hydrogen-producing acidogenic community (S0 to S5) (Figure 1). The strongest community shift occurred between inoculum and H2-producing communities, whereas the H2-producing communities had a more stable structure, sharing several bands in common (Figure 1 appendice). Their structure was mostly driven by the specific conditions common to stages S0 to S5 and different from the inoculum I0 (i.e. shorter HRT and lower pH).

Within the H2-producing communities, the samples were clustered according to the substrate type and concentration. A microbial succession was observed along with the progressive substrate change. Samples fed with null or low glycerol concentration (S0 and S1) clustered together, separated from samples fed with higher glycerol concentration (S2 to S4), indicating the influence of the feeding strategy on the community structure and strongly suggesting a progressive adaptation of the community to increasing glycerol concentrations. Interestingly, the sample corresponding to pure glycerol feeding as sole substrate (S5) exhibited the most

different community structure, clearly discriminated from the samples fed with a mixture of glucose and glycerol (Figure 1). Therefore, the metabolic changes associated to the shift from mixed to pure substrate could be explained by the changes in the community structure. However, the community changes associated with the increase of glycerol concentration within the H2-producing communities revealed by DGGE were mostly linked to slight modifications of band intensities, rather than appearance/disappearance of bands.

The effect of increasing glycerol concentration on total community structure revealed by DGGE was strongly confirmed by the SSCP patterns (Figure 1 and Supplementary Figure 1). Sample clustering was extremely similar, despite some slight differences concerning the intermediate-concentration sample were observed (S2). This consistency between SSCP and DGGE profiles, while the discriminating power of these techniques do not rely on the same characteristics of DNA molecules, confirms the robustness of our methodological approach. It also validates the common assumption made for the analysis of dominant species in low-diversity communities, i.e. that one DGGE band corresponds to one single ribotype and that relative band intensity is proportional to ribotype concentration, even though this assumption is subjected to conceptual limits and potential methodological biases (Loisel et al., 2006).

3.5 Effect of increasing glycerol concentrations on hydrogenase-containing clostridial population

While the 16S approach is not specifically restricted to hydrogen-producing microorganisms in the mixed cultures, the functional hydA approach should give a better estimate of clostridial-type hydrogen producers (32, 34). The presence of bands in all hydA-PCR-DGGE profiles reveals the presence of hydrogen producers from clostridial populations in all samples. Even in the methanogenic inoculum sample where H2 production may be low, a small fraction of 16S rRNA gene sequences were affiliated to clostridia from pyrosequencing data (Table 4).

The clustering obtained from hydA-DGGE and 16S-DGGE profiles were highly similar (Figure 2). Despite some minor clustering differences for intermediate-concentration samples, both methods reveal the same microbial succession and adaptation in response to increasing glycerol concentration. Therefore, the hydA-containing clostridial population and the total bacterial community shifted in a similar way as glycerol concentration increased. However, the structural effect of the highest glycerol concentrations seems to be more important on the hydA-containing fraction of the community than on the total community, since samples corresponding to stages S4 and S5 appeared to be more discriminated in hydA-DGGE clustering than in 16S-DGGE clustering.

The correspondence of sample clustering between 16S- and hydA-targeting fingerprint profiles has also been verified with the SSCP methodology (Figure 2 appendice). *Clostridium* population dynamics therefore reflect the total community dynamics in response to glycerol concentration changes, but this does not imply that *Clostridium* populations would be dominant in the community.

3.6 Link between community structure and environmental variables.

Once verified the consistency between DGGE and SSCP methods as well as 16S and *hydA* analysis, the relationship between community structure and environmental variables was only presented for the 16S-DGGE approach. On the PCA representation that explained more than 90 % of the sample variance, it was observed :

(i) a strong differentiation of the inoculum sample (according to PC1 axis), (ii) a community dynamism clearly differentiating the samples corresponding to low (S0, S1) and high (S2 to S4) glycerol concentrations (according to PC2 axis), and (iii) a clear divergence of the sample corresponding to pure glycerol feeding as sole substrate (S5), all confirming that the influence of glycerol concentration on the community structure was level-dependent (Figure 3A).

Statistically significant correlations were evidenced between the PCA ordination and several environmental variables (p-values < 0.05). Butyrate and valerate production, as well as hydrogen yield when expressed as a percentage of the theoretical yield, were positively correlated to the community structure at high glycerol concentration. Ethanol and acetate production, as well as biomass yield, were positively correlated to intermediate stage community structures, corresponding to medium glycerol concentrations. In contrast, the acetate-to-butyrate ratio (A/B) was associated to low glycerol concentration communities. The correlation between propionate production and community structure was not significant.

3.7 Identification of bacterial populations by 454-pyrosequencing

The microbial populations for each stage of the step-by-step increase strategy were identified by 454 pyrosequencing (Table 4). The samples were represented on PCA ordination according to their microbial composition (Figure 3B). The correlation between the PCA ordination and some discriminant OTUs was evidenced statistically, as discussed below.

The number of analyzed sequences ranged from 2820 to 9432 per sample, distributed into 593 different OTUs. The highest diversity and evenness level were found in the methanogenic inoculum sample (352 OTUs). No any strongly dominant genus or family was found in the inoculum, where the most abundant community members belonging to the Cloacomonas genus, Rikenellaceae family and Rhodanobacter genus represented 13.8 %, 11.2 % and 9.3 % of the total number of sequences, respectively. These important community members were not conserved under the hydrogen-producing conditions. It is interesting to point out that, even though the inoculum came from an anaerobic digester with methanogenic activity, only 2 OTUs were identified as methanogenic Archaea (belonging to Methanosaeta and Methanobacterium genera), representing less than 0.9% of the inoculum community. As expected, these methanogenic Archaea were not found in hydrogen-producing samples.

At the different stages of the operation, the number of OTUs ranged from 40 to 105, suggesting that the specific operating conditions imposed in acidogenic reactors (i.e. lower pH and lower HRT) led to species selection and community simplification, in comparison with the inoculum community.

Interestingly, all the abundant community members in hydrogen-producing communities were very rare in the inoculum and only emerged during hydrogen production. The most abundant genus under all feeding strategies was Prevotella (OTU 1), which was particularly dominant (65 % of the community) in stage 4, i.e. at the highest glycerol and glucose concentrations in the feed. Members of the Veillonellaceae family (OTU 2) were also important members of the community when glycerol was present in the feed (representing from 9.1 to 24.5 % of the community), but they were even more abundant with no glycerol (32.0 % in stage 0). Similarly, Acetobacter (OTU 12) seems to be specific of hydrogen production from pure glucose substrate and represented 16.8 % of the total community. Meanwhile, *Acetobacter sp*. abundance remained below 3.5 % of the community

when glycerol was present in the feed. Therefore, sample S0 -fed with glucose only- differentiates from other samples through a highest percentage of sequences affiliated to the Veillonellaceae family and the Acetobacter genus. On the ordination from sequencing data (Figure 3, right panel), a large number of OTUs were associated with low or intermediate glycerol concentration communities.

Clostridium spp., including OTU 9, were present as minor community members, ie. between 4.8 and 7.1 % of the community, either with glucose substrate only, or with a mixture of glucose and low glycerol concentrations. *C. beijerinckii* (OTU 4) and most of the Clostridiaceae members unidentified at the genus level were more abundant when glycerol was present in the feed, at low concentration (stages S1 and S2). The abundance of these Clostridium species decreased with increasing glycerol concentrations. *C. beijerinckii* is a hydrogen and butanol producer generally isolated from anaerobic sludge (Zhao et al., 2011). Previous studies of hydrogen production systems comparing different Clostridium species for pure culture inoculation, reported ones of the highest hydrogen yields with *C. beijerinckii* pure cultures, depending on the operation conditions (Zhao et al., 2011; Hu et al., 2014). Some *Clostridium sp*., including OTU 3, remained at low abundance (< 8.2 % of the community) during all the H2-producing stages, while they were highly dominant (41.3 % of the community) when glycerol was the only substrate at high concentration (S5). During stage S5, these sequences were more abundant than the previously dominant Prevotella. This specific Clostridium OTU 3 drove the community structure segregation during stage 5 and might be responsible for the high H2 yield performance during stage S5.

Members of the Enterobacteriaceae family (OTU 7) were statistically significant drivers of the community differentiation during stages 4 and 5 (i.e. when glycerol concentration was the highest), even though they represented less than 5 % of the community. Therefore, these members of the Enterobacteriaceae family can be considered as putative hydrogen producers under high glycerol concentrations.

Some community members belonging to Bacteroides and Corynebacterium genus (OTU 8 and OTU 14) appeared transitory under intermediate glycerol concentrations, but their abundance profiles did not follow the glycerol concentration gradient. Contrary to other studies (Goud et al., 2012), Bacillales and Lactobacillales were very minor species, representing always less than 1.3 %.

4. Discussion

4.1 Functional performances

In the present study, the one-step strategy led to biomass washout and unsuccessful H_2 production, but the step-by-step approach was an efficient strategy for biomass adaptation. Step-by-step strategy showed a reduction of biomass yield with glycerol substrate compared to the glucose-feeding conditions (53.9 %-loss factor). This reduction in biomass yield is in agreement with Temudo et al. (2008), who compared glucose versus glycerol fermentation for hydrogen production and observed a 50 % decrease of the biomass yield with glycerol. These differences can be explained by the higher amount of ATP synthesized with glucose than glycerol, which negatively affects the microbial growth, since the growth rate is proportional to the ATP quantity that can be obtained from the mineralization of the energy source in the growth medium.

The hydrogen yields obtained in the present study with glycerol substrate and Step-by-step strategy are comparable with previous results (Table 3). With glycerol substrate, the use of mixed cultures enabled to reach

hydrogen yields between 0.4 and 8 $mmolH_2.g^{-1}_{COD}$ consumed (4-89% of theoretical yield), while the H_2 yields ranged from 3.1 to 7.9 $mmolH_2.g^{-1}_{COD\ consumed}$ with pure cultures of *Enterobacter* and *Klebsiella* genus (34-88% of theoretical yield) (Table 3). The experimental hydrogen yields reached with pure cultures and batch systems are generally higher than the ones reported for mixed cultures. Therefore, it is difficult to compare productivities obtained in this study with literature because there are few studies that have been conducted in a continuous system with glycerol as substrate and also had low yields of hydrogen (Table 3).

The hydrogen production performances reached with the step-by-step strategy with glycerol as sole substrate were better than the ones obtained after a direct shift from glucose to glycerol without progressive transition (one step strategy), which led to unsuccessful H_2 production and a rapid biomass washout. Therefore, the stepwise increase of glycerol ratio in the feed and the progressive decrease of glucose concentration was a successful strategy for the adaptation of biomass to hydrogen production from glycerol. Varrone et al. (2013) observed comparable results with an adaptation strategy called "Enrichment of activity" in successive batch systems with glycerol as sole carbon source. An aerobic sludge was inoculated and the most effective microbial populations were successively selected on the basis of their higher hydrogen production and fresh medium was supplemented after substrate exhaustion, for several months. The authors reported yields of 7.2 $mmol_{H2}.g^{-1}_{COD}$ consumed with an initial glycerol concentration of 20 $g.L^{-1}$. To date, no strategy of adaptation to increasing substrate concentrations has been reported in the context of hydrogen production from glycerol in continuous systems.

In the present study the main metabolites obtained during the step by step strategy were ethanol, acetate and butyrate. In the literature, the main metabolites obtained during hydrogen production from glycerol are usually acetate, ethanol and 1,3-propanediol (Table 3), with different proportions probably coming from different operating conditions and different groups of selected microorganisms. Therefore, butyrate should be positively-associated with the hydrogen yield obtained in this study as been widely reported (Rafrafi et al., 2013).

4.2 Microbial succession

Our results highlighted the shift of microbial community between inoculum and hydrogen-production stages. The divergence between the bacterial communities during the transition from methane to hydrogen production has been previously reported in other acidogenic reactors, through T-RFLP fingerprint analysis (Castelló et al., 2009).

In Step-by-step strategy, The most abundant genus under all feeding strategies was *Prevotella*. *Pretrovella* (non-spore forming and obligate anaerobe) is considered as a late microorganism in sucrose fermentation, which consumes by products such as acetate, succinate or lactate. Recently, Mariakakis et al. (2011) found that *Pretrovella* species produced hydrogen in small amounts. Moreover, this microorganism has been detected by DGGE band sequencing and cloning /sequencing methods in ASBR and CSTR hydrogen producing systems operated under conditions similar to those of the present study (temperature between 35-37 °C, pH 5.3-5.5), fed with sucrose, glucose or starch, inoculated with anaerobic sludge with and without thermal shock pretreatment (Mariakakis et al., 2011; Arroj et al., 2007). *Prevotella* presence was correlated in one case to the highest hydrogen production period (Mariakakis et al. 2011) .

Members of the *Veillonellaceae* family were also important members of the community in this study and were also detected in hydrogen production systems fed with glucose or sugar refinery wastewater, inoculated with anaerobic sludge with and without thermal shock, but their function remains unclear. In some cases they were considered as potential hydrogen consumers, while in other cases they were considered as hydrogen producers or lactate consumers (Hung et al., 2011; Momoe et al., 2012; Won et al., 2013).

The case of the sequences affiliated to the *Clostridiaceae* family as, i.e. well-known hydrogen producers is interesting since they exhibited different abundance profiles according to their taxonomic affiliation (Hu et al., 2014; Hung et al., 2011). *C. beijerinckii* and most of the *Clostridiaceae* members unidentified at the genus level were more abundant at low glycerol concentration in the feed. However, some *Clostridium sp.*, including OTU 3 were highly dominant when glycerol was the only substrate, more abundant than the previously dominant *Prevotella*. Therefore, it can be concluded that all Clostridium species did not participated in the same way in hydrogen production from increasing glycerol concentration and evidenced an interesting shift within the Clostridium genus in relation with the glycerol concentration.

Members of the *Enterobacteriaceae* family were statistically significant drivers of the community differentiation when glycerol concentration was the highest. Members of the *Enterobacteriaceae* family have been isolated from various sources such as agricultural soils, wastewater sludge, cow dung and have been used in hydrogen production studies, exhibiting very different H_2 production capacities (Seol et al., 2008). In mixed cultures fed with glucose and inoculated from active sludge without pretreatment, *Enterobacteriaceae* OTUs have been detected in much lower abundance than *Clostridium* species (Song et al., 2011). In packed bed reactor fed with molasses, *Enterobacteriaceae* developed in a granular form and have been considered as the dominant hydrogen producers, probably because they were not exposed to the competition with heterolactic fermentation bacteria, contrary to what occurred to the *Clostridiaceae* dominant in the attached biofilm (Chojnacka et al., 2011).

4. Conclusions

- Step-by-step strategy was an efficient strategy for community structure adaptation, maintaining around 33% of the theoretical yield independently of the glycerol proportion in the feed.

- Fingerprinting and pyrosequencing results revealed the influence of the feeding strategy on the bacterial community structure and suggested the progressive adaptation of the community, through the emergence and selection of specific species, highly correlated to environmental parameters.

- A microbial succession was observed according to the gradient of glycerol in the feed, with successive dominance of *Veillonellaceae, Prevotella* and *Clostridium sp* identified as major community members putatively involved in efficient hydrogen production from glycerol.

Acknowledgments

The work was founded by Fondecyt 1120659 and the French-Chilean exchange program ECOS-CONICYT project N° C12E06 (ECOMODH2), CORFO project code #09CEII-6991.

References

Akutsu Y, Lee D-Y, Li Y-Y, Noike T (2002) Hydrogen production potentials and fermentative characteristics of various substrates with different heat-pretreated natural microflora. International Journal of Hydrogen Energy 27:1399 - 1405. doi:10.1016/j.ijhydene.2009.04.052

Arooj M, Han S, Kim S, Kim D, Shin H (2007) Sludge characteristics in anaerobic SBR system producing hydrogen gas. Water Research 41: 1177-1184. doi:10.1016/j.watres.2006.11.052

Cabrol L, Malhautier L (2011) Integrating microbial ecology in bioprocess understanding: the case of gas biofiltration. Applied Microbiololy Biotechnology 90: 837-849. doi: 10.1007/s00253-011-3191-9.

Castelló E, García y Santos C, Iglesias T, Paolino G, Wenzel J, Borzacconi L, Etchebehere C (2009) Feasibility of biohydrogen production from cheese whey using a UASB reactor: Links between microbial community and reactor performance. International Journal of Hydrogen Energy 34 (14):5674-5682. doi:10.1016/j.ijhydene.2009.05.060

Chen W, Chen S, Khanal S, Sung S (2006) Kinetic study of biological hydrogen production by anaerobic fermentation. International Journal of Hydrogen Energy 31: 2170-2178. doi:10.1016/j.ijhydene.2006.02.020

Chojnacka A, Błaszczyk M, Szczesny P, Nowak K, Suminska M, Tomczyk-Z_ ak K, Zielenkiewicz U, Sikora A (2011) Comparative analysis of hydrogen-producing bacterial biofilms and granular sludge formed in continuous cultures of fermentative bacteria. Bioresource Technology 102: 10057-10064. doi:10.1016/j.biortech.2011.08.063

Elam C, Gregoire C, Sandrock G, Luzzi A, Lindblad P, Hagen E (2003) Realizing the hydrogen future: the International Energy Agency's efforts to advance hydrogen energy technologies. International Journal of Hydrogen Energy 28(6): 601-607. doi:10.1016/S0360-3199(02)00147-7

González-Pajuelo M, Meynial-Salles I, Mendes F, Andrade J, Vasconcelos I, Soucaille P (2005) Metabolic engineering of Clostridium acetobutylicum for the industrial production of 1,3-propanediol from glycerol. Metabolic Engineering 7: 329-336

Goud, R., Raghavulu, S., Mohanakrishna, G.,Naresh, K., Mohan, S., 2012. Predominance of Bacilli and Clostridia in microbial community of biohydrogen producing biofilm sustained under diverse acidogenicoperating conditions. International journal of hydrogen energy 37, 4068-4076. doi: 10.1016/j.ymben.2005.06.001

Guo XM, Trably E, Latrille E, Carrere H, Steyer JP (2010) Hydrogen production from agricultural waste by dark fermentation: A review. International Journal of Hydrogen Energy 35: 10660-10673. doi:10.1016/j.ijhydene.2010.03.008

Hu C, Giannis A, Chen C, Wang J (2014) Evaluation of hydrogen producing cultures using pretreated food waste. International journal of hydrogen energy 39: 19337-19342. doi:10.1016/j.ijhydene.2014.06.056

Hung C, Chang Y, Chang Y (2011) Roles of microorganisms other than *Clostridium* and *Enterobacter* in anaerobic fermentative biohydrogen production systems – A review. Bioresource Technology 102: 8437-8444. doi:10.1016/j.biortech.2011.02.084

Ito T, Nakashimada Y, Senba K, Matsui T, Nishio N (2005) Hydrogen and Ethanol Production from Glycerol-Containing wastes discharged after biodiesel manufacturing process. Journal of Bioscience and Bioenergineering 100 (3): 260-265. doi: 10.1263/jbb.100.260

Khanal S, Chen W, Li L, Sung S (2004) Biological hydrogen production: effects of pH and intermediate products. Journal of Hydrogen Energy 29(11): 1123-1131. doi:10.1016/j.ijhydene.2003.11.002

Liu F, Fang B (2007) Optimization of bio-hydrogen production from biodiesel wastes by *Klebsiella pneumoniae*. Biotechnology Journal 2: 374-380. doi: 10.1002/biot.200600102

Loisel P, Harmand J, Zemb O, Latrille E, Lobry C, Delgenes J P, Godon JJ (2006) DGE and SSCP molecular fingerprintings revisited by simulation and used as a tool to measure microbial diversity. Environmental Microbiology 8 (4): 720-731. doi: 10.1111/j.1462-2920.2005.00950.x

Mariakakis I, Bischoff P, Krampe J, Meyer C, Steinmetz H (2011) Effect of organic loading rate and solids retention time on microbial population during bio-hydrogen production by dark fermentation in large lab-scale. International journal of hydrogen energy 36: 10690-10700. doi:10.1016/j.ijhydene.2011.06.008

Momoe G, Sader L, Cavalcante de Amorim E, Sakamoto I, Maintinguer S, Saavedra N, Amancio M, Silva E (2012) Performance and composition of bacterial communities in anaerobic fluidized bed reactors for hydrogen production: Effects of organic loading rate and alkalinity. International journal of hydrogen energy 37: 16925-16934. doi:10.1016/j.ijhydene.2012.08.140

Muyzer G, Smalla K (1998) Application of denaturing gradient gel electrophoresis (DGGE) and temperature gradient gelelectrophoresis (TGGE) in microbial ecology. Antonie van Leeuwenhoek International Journal of General and Molecular Microbiology 73(1): 127-141. doi: 10.1023/A:1000669317571

Nakashimada Y, Rachman M, Kakizono T, Nishio N (2002) Hydrogen production of *Enterobacter aerogenes* altered by extracellular and intracellular redox states. International Journal of Hydrogen Energy 27 (11-12): 1399-1405. doi:10.1016/S0360-3199(02)00128-3

Niu K, Zhang X, Tan W, Zhu M (2010) Characteristics of fermentative hydrogen production with *Klebsiella pneumoniae* ECU-15 isolated from anaerobic sewage sludge. International Journal of Hydrogen Energy 35 (1): 71-80. doi:10.1016/j.ijhydene.2009.10.071

Papanikolaou S, Fick M, Aggelis G (2004) The effect of raw glycerol concentration on the production of 1,3-propanediol by *Clostridium butyricum*. Journal of Chemical Technology and Biotechnology 79: 1189-1196. doi: 10.1002/jctb.1103

Quéméneur M, Hamelin J, Latrille E, Steyer JP, Trably E (2011) Functional versus phylogenetic fingerprint analyses for monitoring hydrogen-producing bacterial populations in dark fermentation cultures. International journal of hydrogen energy 36: 3870-3879. doi:10.1016/j.ijhydene.2010.12.100

Rafrafi Y, Trably E, Hamelin J, Latrille E, Meynial-Salles I, Benomar S, Giudici-Orticoni M, Steyer JP (2013) Sub-dominant bacteria as keystone species in microbial communities producing bio-hydrogen. International Journal of Hydrogen Energy 38 (12): 4975-4985. doi:10.1016/j.ijhydene.2013.02.008

Ren N, Guo W, Wang X, Xiang W, Liu B, Wang X, Ding J, Chen Z (2008) Effects of different pretreatment methods on fermentation types and dominant bacteria for hydrogen production. International Journal of Hydrogen Energy 33 (16): 4318-4324. doi:10.1016/j.ijhydene.2008.06.003

Seifert K, Waligorska M, Wojtowski M, Laniecki M (2009) Hydrogen generation from glycerol in batch fermentation Process. International journal of hydrogen energy 34: 3671- 3678. doi:10.1016/j.ijhydene.2009.02.045

Selembo P, Perez J, Lloyd W, Logan B (2009) High hydrogen production from glycerol or glucose by electrohydrogenesis using microbial electrolysis cells. International Journal of hydrogen energy 34: 5373-5381. doi:10.1016/j.ijhydene.2009.05.002

Seol E, Kim S, Raj M, Park S (2008) Comparison of hydrogen-production capability of four different *Enterobacteriaceae* strains under growing and non-growing conditions. International journal of hydrogen energy 33: 5169-5175. doi:10.1016/j.ijhydene.2008.05.007

Siles J, Martín M, Chica A, Martín A (2010) Anaerobic co-digestion of glycerol and wastewater derived from biodiesel manufacturing. Bioresource Technology 101: 6315-6321. doi:10.1016/j.biortech.2010.03.042

Singhabhandhu A, Tezuka T (2010) A perspective on incorporation of glycerin purification process in biodiesel plants using waste cooking oil as feedstock. Energy 35, 2493-2504. doi:10.1016/j.energy.2010.02.047

Song J, An D, Ren N, Zhang Y, Chen Y (2011) Effects of pH and ORP on microbial ecology and kinetics for hydrogen production in continuously dark fermentation. Bioresource Technology 102: 10875-10880. doi:10.1016/j.biortech.2011.09.024

Tapia-Venegas E, Ramírez J, Donoso-Bravo A, Jorquera L, Steyer JP, Ruiz-Filippi G (2013) Bio-hydrogen production during acidogenic fermentation in a multistage stirred tank reactor. International Journal of Hydrogen Energy 38 (5): 2185-2190. doi:10.1016/j.ijhydene.2012.11.077

Temudo M, Poldermans R, Kleerebezem R, Van Loosdrecht M (2008) Glycerol Fermentation by (Open) Mixed Cultures: A Chemostat Study. Biotechnology and Bioengineering. 100 (6): 1088-1098. doi: 10.1002/bit.21857

Trchounian K, Sanchez-Torres V, Wood T, Trchounian A (2011) Escherichia coli hydrogenase activity and H2 production under glycerol fermentation at a low pH. International Journal of Hydrogen Energy. 36 (7): 4323-4331. doi:10.1016/j.ijhydene.2010.12.128

Trchounian K, Trchounian A (2009) Hydrogenase 2 is most and hydrogenase 1 is less responsible for H2 production by Escherichia coli under glycerol fermentation at neutral and slightly alkaline pH. International Journal of Hydrogen Energy. 34: 88398845. doi:10.1016/j.ijhydene.2009.08.056

Varrone C, Rosa S, Fiocchetti F, Giussani B, Izzo G, Massini G, Marone A, Signorini A, Wang A (2013) Enrichment of activated sludge for enhanced hydrogen production from crude glycerol. International Journal of Hydrogen Energy. 38 (3): 1319-1331. doi:10.1016/j.ijhydene.2012.11.069

Wang Y, Qian PY (2009) Conservative Fragments in Bacterial 16S rRNA Genes and Primer Design for 16S Ribosomal DNA Amplicons in Metagenomic Studies. PLoS One 4(10), e7401. doi: 10.1371/journal.pone.0007401

Won S, Baldwin S, Lau A, Rezadehbashi M (2013) Optimal operational conditions for biohydrogen production from sugar refinery wastewater in an ASBR. International journal of hydrogen energy. 38: 13895-13906. doi:10.1016/j.ijhydene.2013.08.071

Wu K, Lin Y, Lo Y, Chen C, Chen W, Chang J (2011) Converting glycerol into hydrogen, ethanol, and diols with a *Klebsiella sp.*HE1 strain via anaerobic fermentation. Journal of the Taiwan Institute of Chemical Engineers. 42 (1): 20-25. doi:10.1016/j.jtice.2010.04.005

Zhao X, Xing D, Fu N, Liu B, Ren N (2011) Hydrogen production by the newly isolated *Clostridium beijerinckii* RZF-1108. Bioresource Technology. 102: 8432-8436. doi:10.1016/j.biortech.2011.02.086

Fig 1. UPGMA clustering based on Bray Curtis similarity from 16S DGGE (left) and 16S SSCP (right) profiles. I0 is the methanogenic inoculum. S0 to S5 correspond to steady states of the progressive increase of glycerol concentration in the step-by-step strategy, as stated in Table 1. The scale bar indicates 5 % of dissimilarity.

Fig 2. UPGMA clustering based on Bray Curtis similarity from 16S (A) and *hydA* (B) DGGE profiles. I0 is the methanogenic inoculum. S0 to S5 correspond to steady states of the progressive increase of glycerol concentration in the step-by-step strategy, as stated in Table 1. The scale bar indicates 5 % of dissimilarity.

Fig 3.Principal Component Analyses (PCA) of microbial community patterns generated by 16S-DGGE analysis (left panel) and 454 pyrosequencing (right panel). In the left panel, the arrows represent the significant (*) correlations with environmental variables (But: butyrate; Val: valerate; Eth: ethanol; Ace: acetate; H2 Yield: hydrogen yield expressed in percentage of the theoretical yield; Biomass: biomass yield; A/B: acetate to butyrate ratio), calculated as stated in Table 2. In the right panel, the arrows represent the most discriminant OTUs from 454 sequencing. In both representations, the size of the circles is proportional to glycerol percentage in the feed, I0 is the methanogenic inoculum, and S0 to S5 correspond to steady states of the progressive increase of glycerol concentration in the step-by-step strategy, as stated in Table 1. The percentages of variance expressed in the first and second axes of PCA ordinations are displayed.

Fig 1 (Appendix). UPGMA clustering based on Bray Curtis similarity from 16S DGGE and 16S SSCP profiles of step-by-step strategy. S0 until S5 indicate the day in steady state of a stage at Increased Steps experiment, and I0 indicated the initial anaerobic sludge used as inoculum. The alignments of bands were performed using Gel Compar II software and peaks were performed using the R software with an internal standard and areas were normalized, the similarities of the samples were analyzed by method Bray Curtis Buy with R program.

Fig 2 (Appendix). UPGMA clustering based on Bray Curtis similarity from *hydA* DGGE and *hydA* SSCP profiles of step-by-step strategy. S0 until S5 indicate the day in steady state of a stage at Increased Steps experiment, and I0 indicated the initial anaerobic sludge used as inoculum. The alignments of bands were performed using Gel Compar II software and peaks were performed using the R software with an internal standard and areas were normalized, the similarities of the samples were analyzed by method Bray Curtis Buy with R program.

Table 1. Experimental design of two types of feeding strategy: one-step strategy and step-by-step strategy.

Experiment	Stage	Number of HRTs	Period (Days)	Glycerol concentration (% COD)	Glucose concentration (% COD)	Total COD ($g_{COD}.L^{-1}$)
One-step strategy	-	20	0-10	100	0	6.3 ± 0.1
Step-by-step strategy	**S0**	22	0-11	0	100	5.4 ± 0.3
	S1	30	12-27	52	48	5.0 ± 0.3
	S2	32	28-44	60	40	6.0 ± 0.4
	S3	28	45-59	65	35	7.5 ± 0.4
	S4	32	60-76	71	29	8.6 ± 0.3
	S5	34	77-94	100	0	6.1 ± 0.1

Table 2. Performance indicators of hydrogen production during the different stages of the step-by-step strategy, including glycerol and glucose degradation efficiency, hydrogen yield and productivity, biomass yield and by-products production. Average values and standard deviations (in parenthesis) were calculated during steady state of the continuous operation during 20 HTRs.

Parameter	Unit	Stages					
		0	1	2	3	4	5
Glycerol RE	%	-	55.3 *(5.9)*	50.3 *(4.4)*	66.6 (4.8)	70.4 *(6.1)*	69.8 *(1.3)*
Glucose RE	%	95.6 *(1.4)*	86.6 *(2.2)*	86.6 *(1.7)*	87.5 *(2.0)*	87.2 *(1.2)*	-
H_2 Yield	$mmol_{H2}.g_{COD}^{-1}$	6.1 (1.2) [a]	4.5 *(0.6)*	5.4 *(1.2)*	4.6 *(0.9)*	3.7 *(1.1)*	3.2 *(1.1)* [b]
H_2 Yield	% [C]	29 *(6)*	31 *(5)*	40 *(9)*	35 *(6)*	28 *(8)*	36 *(12)*
H_2 Productivity	$ml_{H2}.l^{-1}h^{-1}$	61.9 *(12.2)*	31.4 *(3.8)*	41.7 *(6.2)*	50.1 *(10.3)*	46.7 *(10.3)*	24.7 *(9.1)*
Biomass Yield	$mg_{VSS}.g_{COD}^{-1}$	223.5 *(26)*	210.6 *(17)*	238.5 *(22)*	171.7 *(23)*	129.3 *(13)*	145.3 (28)
Acetate	$\%COD_m$	40.8 *(2.1)*	39 *(1.7)*	41.5 *(2.2)*	36.9 *(0.4)*	36.3 *(0.8)*	29.3 *(3.4)*
Ethanol	$\%COD_m$	35.6 *(1.2)*	35.3 *(6.9)*	25.7 *(1.2)*	26.3 *(0.1)*	23.5 *(0.6)*	29.8 *(1.1)*
Butyrate	$\%COD_m$	20 *(2.3)*	9 *(4.8)*	16.2 *(1.5)*	19.7 *(0.9)*	23.1 *(0.4)*	26.7 *(4.2)*
Propionate	$\%COD_m$	3.6 *(0.7)*	11.5 *(2.5)*	8.5 *(1.3)*	6.2 *(1.3)*	9.3 *(0.3)*	5.6 *(2.4)*
Valerate	$\%COD_m$	0	5.2 *(0.5)*	8.1 *(0.6)*	10.8 *(0.2)*	7.9 *(0.7)*	8.6 *(2.5)*
Total COD	$g_{COD}.L^{-1}$	2.3 *(0.2)*	3.7 *(0.5)*	4.8 *(0.3)*	5.1 *(0.1)*	5.7 *(0.1)*	1.5 *(0.0)*
A/B	$g_{COD}.g_{COD}^{-1}$	4.13	1.88	1.57	2.05	2.54	1.09

[a] For pure glucose feeding, this yield corresponds to 1.2 ± 0.2 $mol_{H2}.mol^{-1}_{glucose\ consumed}$

[b] For pure glycerol feeding, this yield corresponds to 0.4 ± 0.1 $mol_{H2}.mol^{-1}_{glycerol\ consumed}$.

[c] The hydrogen yield is expressed as the percentage of the maximal theoretical yield, depending on the substrate considered (see Material and Method section).

Total COD: total metabolite concentration expressed in COD.

$\%COD_m$: metabolite concentration expressed in percentage of total measured metabolite concentrations (in COD).

A/B: ratio of acetate to butyrate concentrations, expressed in COD.

Table 3. Hydrogen yields from glycerol fermentation reported in the literature. The main operating conditions and the most abundant metabolites are also indicated.

	Inoculum	Inoculum treatment	Operating conditions	Glycerol concentration ($g.L^{-1}$)	H_2 yield ($mol_{H2}.mol^{-1}_{glycerol}$)	H_2 yield ($mmol_{H2}.g^{-1}_{COD}$)	Main metabolites	Reference
Mixed cultures	Anaerobic sludge and acidogenic sludge	Low HRT	Chemostat HRT 10h pH 8.0 T 30°C	4	0.05	0.4	Ethanol and 1,3 propanediol	Temudo *et al.* (2008)
	Kitchen Waste	Thermal shock	Batch pH 6.5 T 35°C	4	0.11	1.0	Aceticacid and 1,3 propanediol	Akutsu *et al.* (2009)
	Soil	Thermal shock	Batch pH 6,5 T 35°C	3	0.28	2.5	Acetate and ethanol	Selembo *et al.*(2009)
	Anaerobic sludge	Thermal shock	Batch pH 6 37°C	10	0.41	3.7	1,3 propanediol and lactate	Seifert *et al.*(2009)
	Activity sludge from wastewater treatment plant	Enrichment	Batch PH initial 8 T 37°C	15	0.9	8.0	NR	Varrone *et al.*(2013)
	Anaerobic sludge	Low HRT	Chemostat HRT 12 h pH 5,5 T 37°C	5	0.4	3.2	Ethanol and acetate	This study
Pure Cultures	*Klebsiella Ssp.*	NT	Batch pH 6.0 T 35°C	50	0.35	3.1	1,3 propanediol and ethanol	Wu *et al.*(2011)
	Enterobacter aerogenes	NT	Batch pH6,8 T 37°C	10	0.89	7.9	Ethanol	Ito *et al.*(2005)
	Enterobacter aerogenes HU-101	NT	Batch pH 6,3 T 37°C	10	0.62	5.5	Ethanol	Nakashimada *et al.*(2002)

	Inoculum	Inoculum treatment	Operating conditions	Glycerol concentration ($g.L^{-1}$)	H_2 yield ($mol_{H2}.mol^{-1}_{glycerol}$)	H_2 yield ($mmol_{H2}.g^{-1}_{COD}$)	Main metabolites	Reference
	Clostridium acetobutylicum ATCC 824	NT	Chemostat (HRT : NR) pH 6,5 T 35°C	10	<0.1	0	1,3 propanediol and butyrate	Gonzalez *et al.*(2005)
	Klebsiella pneumoniae	NT	Batch pH, T°: NR	20	0.53	4.7	Ethanol	Liu *et al.*(2007)

NR: not reported; NT: no treatment

Table 4. Identification of the bacterial populations by pyrosequencing of 16S rRNA gene. Percentage in communities are displayed. Only the groups of sequences with a relative abundance higher than 0.1% in at least one sample are presented. A grey scale proportional to sequence abundances is used for a better readability.

	Samples			I0	S0	S1	S2	S3	S4	S5	Total
	Number of sequences			8120	2820	6432	3168	5261	9432	3579	38812
	Number of OTUs			352	53	105	70	83	79	40	**593**
	Higher taxonomic rank	**Genus**	**Number of OTUs**	**Sequence relative abundance. per sample (% all sequences)**							**Most representative OTU**
Phylum Bacteroidetes	*Prevotellaceae*	*Prevotella*	**12**	-	35.2	42.3	44.7	47.8	65.0	32.9	*OTU 1*
	Rikenellaceae	*Unclassified*	**1**	11.2	-	-	-	-	-	-	*OTU 6*
	Bacteroidaceae	*Bacteroides*	**4**	-	-	1.1	1.6	5.3	0.5	0.1	*OTU 14*
	Porphyromonadaceae	*Proteiniphilum*	**11**	3.8	-	-	-	-	-	-	*OTU 19*
	Other Bacteroidales		**9**	1.2	0.8	0.1	0.2	1.5	-	-	
	Cryomorphaceae	*Fluviicola*	**2**	6.0	-	-	-	-	-	-	*OTU 13*
	Other Flavobacteriales		**12**	1.4	0.1	0.6	0.7	1.5	0.4	-	
	Chitinophagaceae	Unclassified	**2**	2.7	-	-	-	-	-	-	*OTU 16*
	Other Sphingobacteriales		**5**	0.5	-	-	-	0.1	-	-	
	Other *Bacteroidetes* (unclassified)		**18**	1.9	-	0.1	0.3	1.8	0.3	0.3	
Phylum Firmicutes	*Veillonellaceae*		**34**	-	32.0	9.1	12.9	24.5	16.5	14.9	*OTU 2*
	Bacilli (Bacillales and Lactobacillales)		**19**	1.5	1.0	0.6	1.3	0.5	0.9	0.5	
	Ruminococcaceae		**20**	0.2	-	0.1	0.5	1.3	0.4	0.1	
	Clostridiaceae	*Clostridium sp.*	**9**	-	0.4	8.2	5.3	2.2	7.8	41.3	*OTU 3*
	Clostridiaceae	*Clostridium beijerinckii*	**13**	-	0.3	17.2	11.6	0.1	0.5	0.8	*OTU 4*
	Clostridiaceae	*Clostridium sp.*	**9**	-	7.0	7.1	4.8	-	0.1	0.2	*OTU 9*
	Other Clostridiaceae unclassified		**74**	0.1	2.1	7.4	6.8	0.3	1.5	1.6	*OTU 11*

Phylum Spirochaetae	*Spirochaetes*	*Cloacamonas*	**3**	13.8	-	-	-	-	-	-	*OTU 5*
	Other *Spirochaetes*		**7**	0.3	-	-	-	-	-	-	
	Rhodobiaceae	*Parvibaculum*	**2**	2.7	-	-	-	-	-	-	*OTU 17*
	Acetobacteraceae	*Acetobacter*	**2**	-	16.8	-	0.3	0.2	0.2	3.5	*OTU 12*
	Other *Alphaproteobacteria*		**46**	5.0	-	-	0.1	0.1	0.1	0.1	
	Comamonadaceae		**20**	5.4	0.3	0.1	0.3	0.3	-	-	*OTU 15*
	Hydrogenophilaceae	*Thiobacillus*	**2**	2.2	-	-	-	-	-	-	
	Other Betaproteobacteria		**34**	4.4	-	-	0.1	0.3	0.1	-	*OTU 18*
	Deltaproteobacteria		**16**	1.8	-	-	-	-	-	-	
	Enterobacteriaceae		**21**	0.0	1.7	1.3	2.1	3.4	4.7	3.2	*OTU 7*
	Moraxellaceae	*Perlucidibaca*	**5**	2.4	-	-	-	-	-	-	*OTU 20*
	Xanthomonadaceae	*Rhodanobacter*	**7**	9.3	-	-	-	-	-	-	*OTU 10*
	Xanthomonadaceae	*Thermomonas*	**2**	2.4	-	-	-	-	-	-	
	Xanthomonadaceae	*Others*	**13**	3.3	0.2	0.1	-	0.1	-	-	
Phylum Proteobacteria	Other Gammaproteobacteria		**25**	1.6	1.6	0.5	0.6	1.1	0.4	0.2	
Phylum Actinobacteria	Corynebacteriaceae	Corynebacterium	**5**	0.0	0.2	3.8	5.3	6.7	0.7	0.1	*OTU 8*
	Other Actinobacteria		**20**	1.1	0.1	0.1	0.2	0.2	-	0.1	
	Thermotogaceae		**5**	1.2	-	-	-	-	-	-	
	Acidobacteria		**2**	0.2	-	-	-	-	-	-	
	Chloroflexi		**3**	0.4	-	-	-	-	-	-	
	Planctomycetes		**12**	0.6	-	-	-	-	-	-	
Other Bacteria	*Bacteria/Unclassified*		**85**	9.9	0.1	0.1	0.1	0.1	0.1	0.1	
	Euryarchaeota	*Methanosaeta*	**1**	0.8	-	-	-	-	-	-	
Archaea	*Euryarchaeota*	*Methanobacterium*	**1**	0.1	-	-	-	-	-	-	

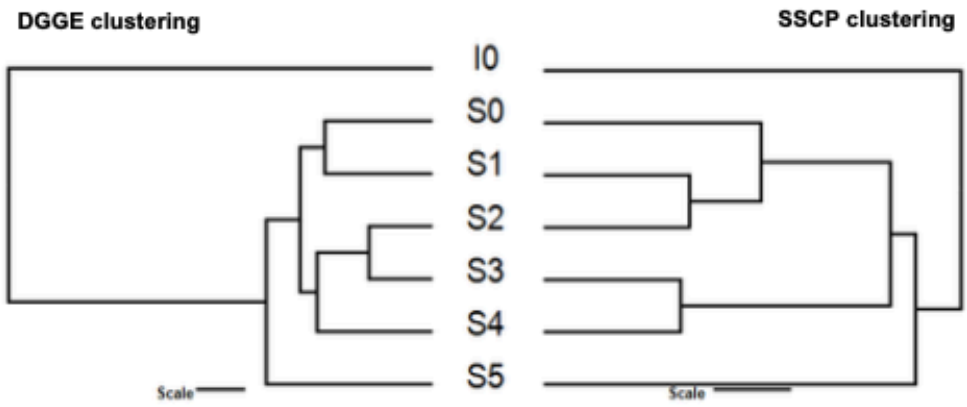

Fig 1. UPGMA clustering based on Bray Curtis similarity from 16S DGGE (left) and 16S SSCP (right) profiles. I0 is the methanogenic inoculum. S0 to S5 correspond to steady states of the progressive increase of glycerol concentration in the step-by-step strategy, as stated in Table 1. The scale bar indicates 5 % of dissimilarity.

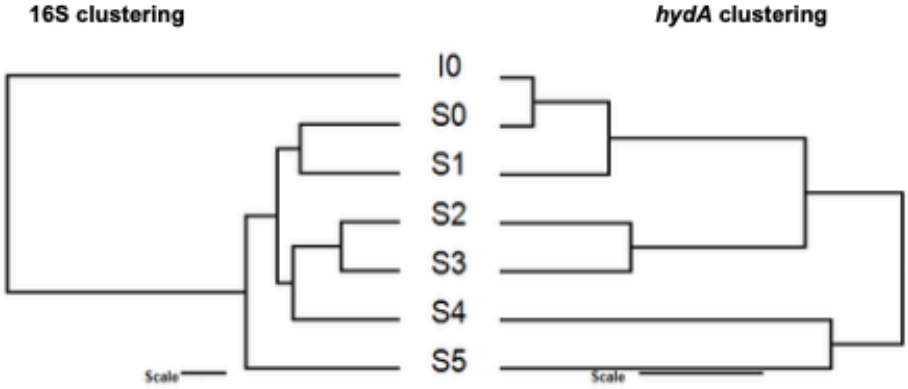

Fig 2. UPGMA clustering based on Bray Curtis similarity from 16S (A) and *hydA* (B) DGGE profiles. I0 is the methanogenic inoculum. S0 to S5 correspond to steady states of the progressive increase of glycerol concentration in the step-by-step strategy, as stated in Table 1. The scale bar indicates 5 % of dissimilarity.

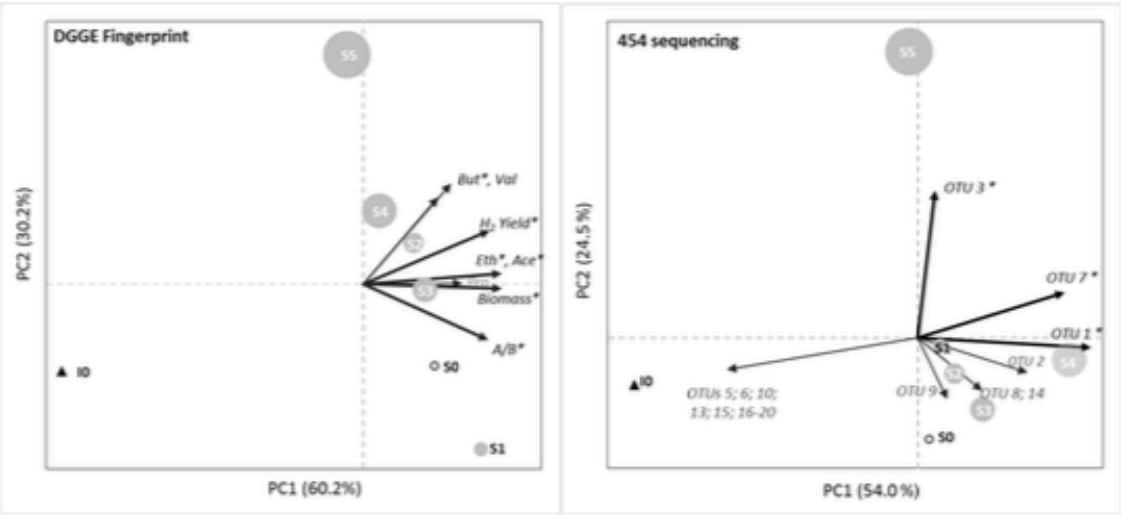

Fig 3. Principal Component Analyses (PCA) of microbial community patterns generated by 16S-DGGE analysis (left panel) and 454 pyrosequencing (right panel). In the left panel, the arrows represent the significant (*) correlations with environmental variables (But: butyrate; Val: valerate; Eth: ethanol; Ace: acetate; H2 Yield: hydrogen yield expressed in percentage of the theoretical yield; Biomass: biomass yield; A/B: acetate to butyrate ratio), calculated as stated in Table 2. In the right panel, the arrows represent the most discriminant OTUs from 454 sequencing. In both representations, the size of the circles is proportional to glycerol percentage in the feed, I0 is the methanogenic inoculum, and S0 to S5 correspond to steady states of the progressive increase of glycerol concentration in the step-by-step strategy, as stated in Table 1. The percentages of variance expressed in the first and second axes of PCA ordinations are displayed.

Applied Microbiology and Biotechnology

Adaptation of acidogenic sludge to increasing glycerol concentrations for bio-hydrogen production

E. Tapia[1*], L. Cabrol[1,2], B. Brandhoff[1], J. Hamelin[3], E. Trably[3], JP Steyer[3], G. Ruiz-Filippi[1]

[1] *Escuela de Ingeniería Bioquímica, Pontificia Universidad Católica de Valparaíso*, Avenida Brasil 2085, Valparaíso, Chile.

[2]Fraunhofer Chile Research Foundation – Center for Systems Biotechnology, FCR-CSB. Mariano Sánchez Fontecilla 310, Las Condes, Santiago, Chile

[3]INRA, UR 0050, Laboratoire de Biotechnologie de l'Environnement, Avenue des Etangs F-11100, Narbonne, France.

**Corresponding author. Escuela de Ingeniería Bioquímica, Pontificia Universidad Católica de Valparaíso, Av Brasil 2085, Valparaíso, Chile. Tel.: +56 (32)2372025*

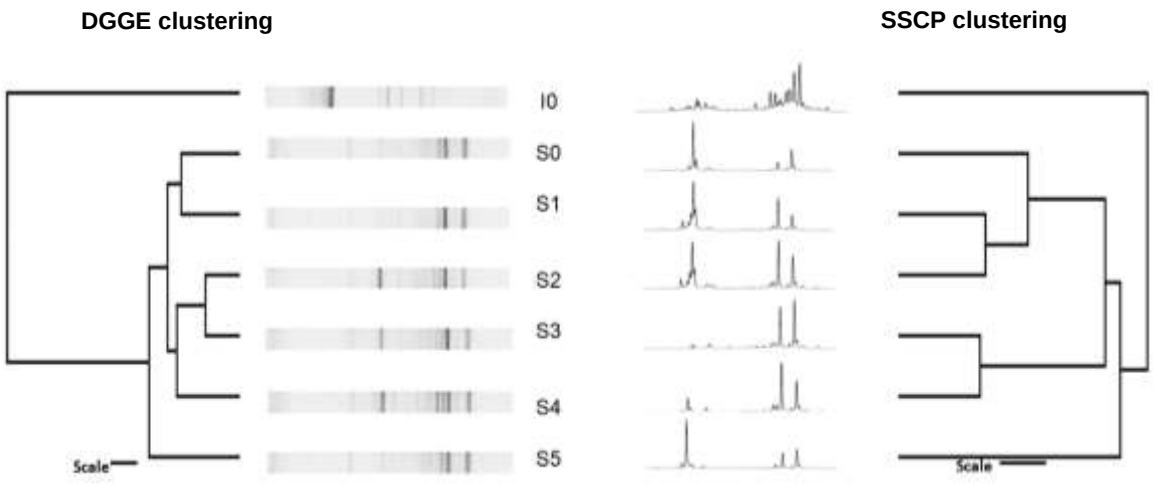

Fig S1. UPGMA clustering based on Bray Curtis similarity from 16S DGGE and 16S SSCP profiles of step-by-step strategy. S0 until S5 indicate the day in steady state of a stage at Increased Steps experiment, and I0 indicated the initial anaerobic sludge used as inoculum.

The alignments of bands were performed using Gel Compar II software and peaks were performed using the R software with an internal standard and areas were normalized, the similarities of the samples were analyzed by method Bray Curtis Buy with R program.

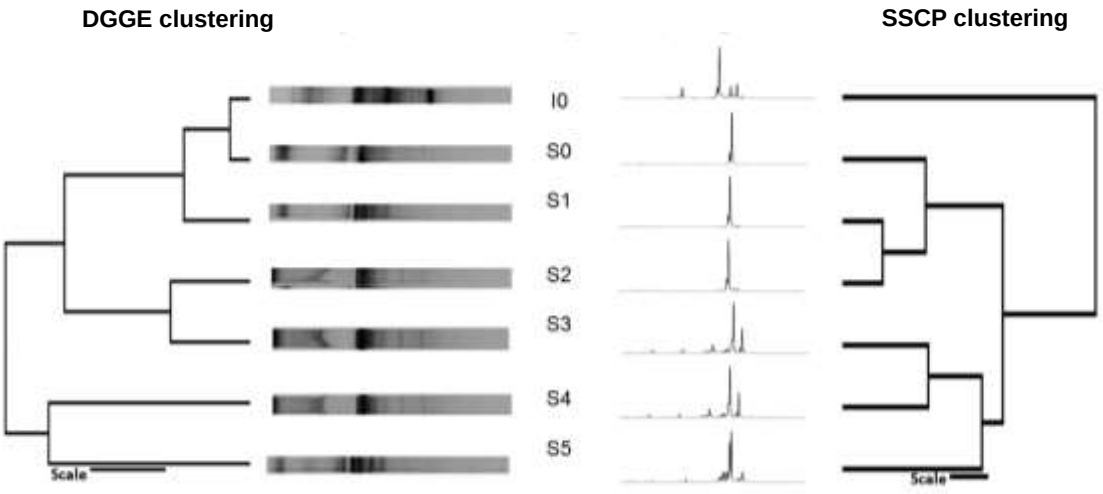

Fig S2. UPGMA clustering based on Bray Curtis similarity from *hydA* DGGE and *hydA* SSCP profiles of step-by-step strategy. S0 until S5 indicate the day in steady state of a stage at Increased Steps experiment, and I0 indicated the initial anaerobic sludge used as inoculum. The alignments of bands were performed using Gel Compar II software and peaks were performed using the R software with an internal standard and areas were normalized, the similarities of the samples were analyzed by method Bray Curtis Buy with R program.